Enhancing CO_2 Decomposition and Oxygen Removal via Ceramic hollow Fibers in a Microwave Plasma Torch

K. Wiegers[1], A. Schulz[1], M. Walker[1], F. Buck[2], T. Schiestel[2] and G. Tovar[1]
[1] *Institute of Interfacial Process Engineering and Plasma Technology, University of Stuttgart, Stuttgart, Germany*
[2] *Fraunhofer Institute for Interfacial Engineering and Biotechnology, Fraunhofer IGB, Stuttgart, Germany*

Abstract: CO_2 is decomposed into CO and O_2 in a plasma torch. The CO_2 conversion can be increased significantly by a factor of 4 to 21% by optimizing the gas management through a nozzle. Since only the CO is desired as a basic chemical, the simultaneously produced O_2 must be separated from the gas mixture. The gas separation is achieved by introducing ceramic hollow fibers, made of $La_{0.6}Ca_{0.4}Co_{0.5}Fe_{0.5}O_{3-\delta}$ (LCCF). In addition, the permeated oxygen flow can be increased to 4.6 mL·min^{-1} per fiber in the nozzle configuration.

Keywords: CO_2 Conversion, Ceramic Hollow fibers, Oxygen Separation, Plasma Reactor

1. Introduction

Mankind nowadays is strongly affected by ongoing climate change, mainly caused by the increasing emission of carbon dioxide (CO_2). CO_2 is a very stable molecule, but it can be activated by a plasma process, which converts CO_2 into the value-added chemical molecule CO [1]. Currently, the basic chemical CO is produced by and from fossil fuels. Nevertheless, various alternative methods are being studied intensively because of the climate crisis. A well-known process is the electrochemical reduction of CO_2 [2]. Another method is the dissociation of CO_2 in a plasma process. However, the CO_2 conversion to CO in the plasma must be increased to become competitive with electrolysis. Therefore, the back reaction to CO_2 has to be suppressed to improve the efficiency of the plasma process. For this purpose, the gas management is enhanced by nozzles. There, the hot plasma core and the cold gas envelope are forced to pass together through a restriction with a diameter of 10 and 5 mm, respectively.

In order to achieve only CO, the simultaneously produced O_2 must be separated from the gas mixture. In order to do so, oxygen-conducting ceramic hollow fibers can be used. These ceramics are made of the so-called MIEC (mixed ionic and electronic conductivity) materials. The first and well-investigated ceramic is $La_{0.58}Sr_{0.4}Co_{0.2}Fe_{0.8}O_{3-\delta}$ by Tereoka [3]. The temperature stability and chemical resistance against the CO_2 and CO atmosphere in the plasma membrane reactor is essential. Therefore, the A site cations are changed, or a dual-phase material is used to increase temperature and chemical stability. In the current work, $La_{0.6}Ca_{0.4}Co_{1-x}Fe_xO_{3-\delta}$ with $x = 0.2$ and 0.5 (LCCF6482 and LCCF6455) has been used as material for the ceramic fibers.

Through the change in gas management, as much plasma area as possible is made available for the surface-sensitive separation process. The current work investigates the changes in conversion and oxygen permeation through variations in gas management.

2. Experimental Setup

Plasma device

In Fig.1 a schematic sketch of the plasma torch is shown. The microwaves produced by the magnetron are coupled via a rectangular waveguide into the resonator structure [4]. The resonator structure consists of a coaxial resonator, which is essential for the ignition of the plasma, and the cylindrical resonator, which is important for the continuous operation of the plasma. The gas is fed in via four tangential inlets. This configuration leads to a rotational flow, where the hot plasma core is stabilized in the middle of the quartz glass tube, and a cold envelope is formed around.

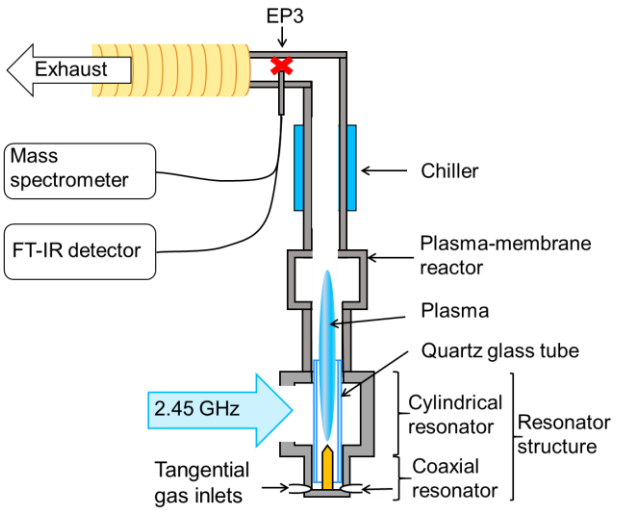

Fig. 1: Schematic sketch of the plasma torch in the free jet configuration.

In Fig.1 the gas swirls up without distortion through additional components. This configuration is called free jet configuration. Fig.2 shows the schematic sketch of the changes in gas management. A nozzle with a smaller central section (in this work 5 and 10 mm, respectively) is mounted on top of the resonator structure. Both nozzles have an opening angle of 60°. The setup with the nozzles is called nozzle configuration. The idea is that the gas is cooled down rapidly after the restriction and so the back-reaction from CO and O_2 to CO_2 is suppressed. The expansion of the gas once it passes after the restriction increases the surface area of the fibers that come into contact with the plasma.

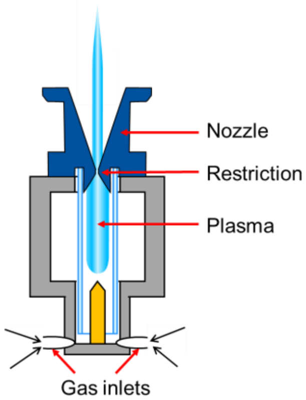

Fig. 2: Nozzle configuration.

Conversion and Energy Efficiency

The conversion of the plasma torch is determined by means of two independent diagnostics, mass spectrometry (MS) and Fourier-transform infrared absorption spectroscopy (FT-IR). The extraction point for the gas analysis is behind the chiller and is indicated as EP3 in Fig.1. In Wiegers et al. [5] it is shown that in the free jet configuration the gas at the extraction point (EP3) is totally mixed and cooled down to room temperature.

Oxygen permeation setup

For oxygen separation, ceramic hollow fibers are used. The hollow fiber geometry has the advantage of possessing a high specific surface area. The LCCF fibers are manufactured at the Fraunhofer IGB. The spinning procedure is explained by Buck et al. [6]. The oxygen permeation setup is shown in Fig.3. The fibers are placed in the flange's holes in the plasma membrane reactor. For the oxygen permeation measurements, a sweep gas (in this work, the sweep gas is argon, $F(\mathrm{Ar})$ = 140 mL·min^{-1}) is introduced into the fiber. In the hot area (T>700 °C), the oxygen permeates inside the fiber. Downstream, an oxygen detector (Zirox SGM7) is placed. There the oxygen concentration c_{O_2} of the sweep gas is determined in ppm. The permeated O_2 flow $F(O_2)$ is calculated with:

$$F(O_2) = c_{O_2} \cdot 10^{-6} \cdot \frac{F(Ar)}{1 - c_{O_2} \cdot 10^{-6}}. \qquad (1)$$

To resolve the oxygen permeation spatially, a blind flange with pre-defined positions is mounted at both ends of the plasma membrane reactors. The position in the middle is called middle position (MP). The spacing between positions is equal to 0.5 cm. The oxygen permeation of a single fiber at MP has been shown elsewhere [7]. An increasing microwave (MW) power leads to higher temperature in the plasma membrane reactor. The CO_2 flow in the reactor is kept constant at 6 L·min^{-1}.

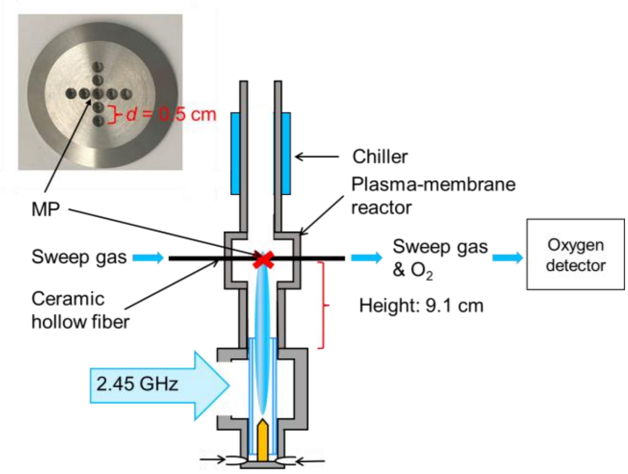

Fig. 3: Schematic setup for oxygen permeation.

Numerical cold gas simulations

The numerical simulations of the cold gas flows in the different nozzle configurations are carried out with the finite element software COMSOL Multiphysics®. For the computational fluid dynamics (CFD) simulation, the geometry of the free jet configuration and the two nozzles configuration are implemented in the model. The simulations are based on the Navier stokes equations:

$$\frac{\partial \rho}{\partial t} + \nabla \cdot \rho \vec{v} = 0 \qquad (1)$$

$$\rho \frac{\partial \vec{v}}{\partial t} + \rho(\vec{v} \cdot \nabla)\vec{v} = \nabla \cdot (-p\boldsymbol{I} + \tau) + \vec{\boldsymbol{F}} \qquad (2)$$

with ρ = density, $\vec{v}$ = velocity, $\boldsymbol{I}$ = unit tensor, τ = viscous stress tensor, $\vec{\boldsymbol{F}}$ = volume force vector. Afterwards the simulation is solved with the turbulent k-ω-model.

3. Results and Discussion

Numerical cold gas simulation

The results of the CFD simulations are displayed in Fig. 4. The four gas inlets originate a rotational gas flow that extends itself upwards. In the nozzle configurations, the gas velocity increases rapidly in the restriction, and afterward, the gas velocity decreases again. In the expanding region of the nozzle, gas turbulences can be observed.

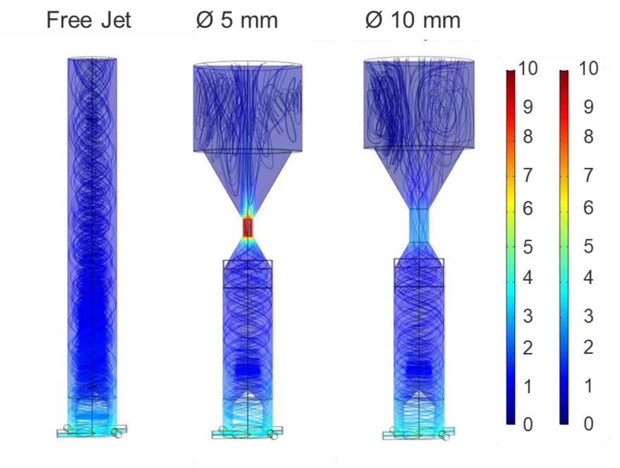

Fig. 4: Cold gas velocity of the free jet configuration and the nozzle configuration with a restriction of 5 and 10 mm, respectively.

CO_2 conversion in the free jet and nozzle configuration

Fig.5 shows the measured conversion for the free jet configuration in black. The maximal conversion is equal to 8% at a specific energy input (SEI) of 1.5 eV·molecule^{-1}. The conversions of the nozzle with the 5 and 10 mm restrictions are shown in red and blue, respectively. The conversion values of the 10 mm restriction are higher than those of the free jet configuration, while the 5 mm restriction shows the best conversion values. The nozzle with the restriction of 5 mm reaches a conversion of 21% at a SEI of 2.1 eV·molecule^{-1}. For these operating parameters, the conversion is increased by a factor of 4 compared to the free jet configuration.

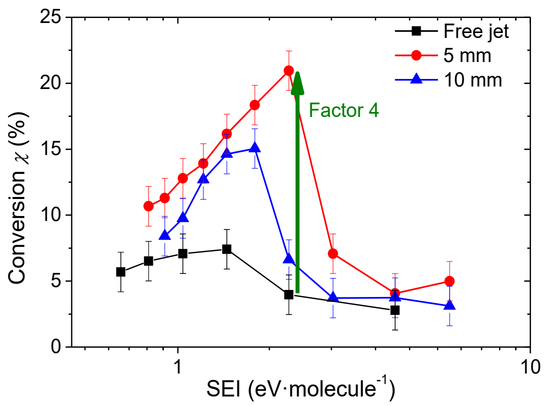

Fig. 5: Conversion measurements.

Hecimovic et al. [8] explained in a comparable plasma torch that the nozzle forces the hot gas and the cold one from the envelope to mix together, resulting in a cooling effect and thus reducing the CO recombination with oxygen into CO_2. In the gas simulations (Fig. 4), the nozzle with the 5 mm restriction has the highest velocity and the greatest turbulences, one assumption would be that this suppresses the back reaction the best.

Spatially resolved oxygen permeation for LCCF6482 in the free jet configuration

Fig. 6 shows an experimental setup in which four fibers are mounted above each other in the membrane reactor. The glowing of the fibers displays hints about their temperature distribution. The fiber in the lowest position shows the brightest glowing and so the highest temperature. The temperature profiles along the same fiber are all gaussian-like [7].

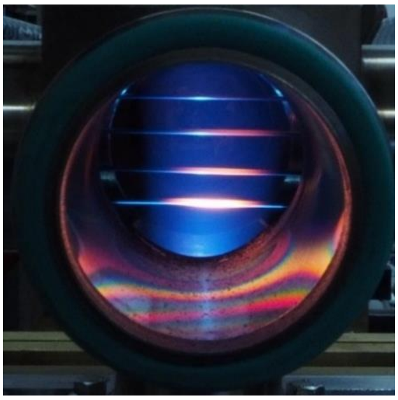

Fig. 6: Four fibers in the plasma-membrane-reactor in the free jet configuration.

The different temperatures for the fibers at a microwave (MW) power of 0.76 kW lead to different oxygen permeation values. This spatially resolved oxygen permeation for the different positions is shown in Fig 7. The permeated oxygen depends strongly on the position inside the plasma-membrane-reactor. The vertically resolved oxygen permeation is the highest in the lowest position, where the highest temperature is measured. With increasing height, the permeated oxygen amount decreases. If the horizontally resolved permeated oxygen is considered, the permeated oxygen is the highest for the fiber in the middle and goes down when moving to the sides.

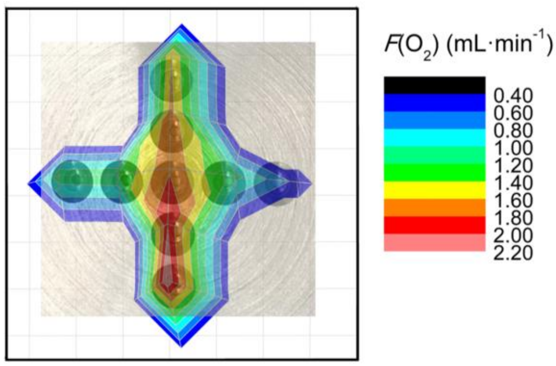

Fig. 7: Permeated oxygen flow of LCCF6482 fibers for different positions for a MW power of 0.76 kW.

Oxygen permeation in the nozzle configuration

Experimental results show that the overall conversion is increased by using a nozzle. In this case, the permeated oxygen amount in the nozzle configuration is compared to the free jet configuration. The gas flow for the plasma is kept constant at 6 slm CO_2. In Fig. 8, the oxygen permeating inside the fiber is plotted against the MW power. The permeated oxygen amount is steadily higher in the free jet configuration than in the nozzle configuration. At a MW power higher than 0.76 kW, however the LCCF6455 fiber is unstable in the free jet configuration. The reason is that temperatures above 1200 °C are reached and the fiber starts to melt. In the nozzle configuration, instead, the LCCF6455 fiber is stable up to a MW power of 1.13 kW, with a corresponding permeated oxygen amount equal to 4.6 $mL \cdot min^{-1}$.

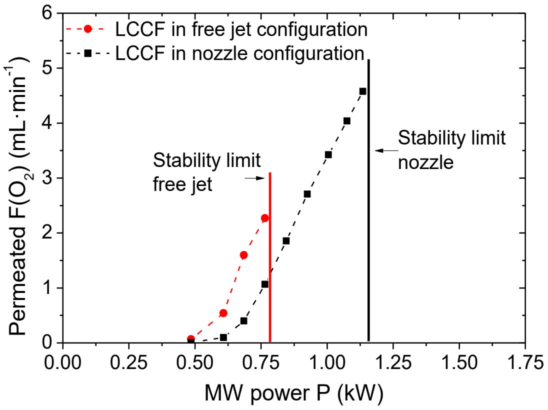

Fig. 8: Oxygen permeation of LCCF6455 fibers in the nozzle and in the free jet configuration.

4. Conclusion

The maximal overall conversion in the free jet configuration is around 8%. This value can be increased when the gas management is changed by means of a nozzle. For the nozzle with a 5 mm restriction, the maximal conversion is 21%. The oxygen permeation of LCCF6455 fibers has been determined in the free jet configuration and for the nozzle with 5 mm. The amount of permeated oxygen through a fiber is strongly dependent on the temperature. So, the fiber nearest to the plasma zone also shows the highest permeation values. At the MP in the free jet configuration, the oxygen permeation is around 1.8 $mL \cdot min^{-1}$ for LCCF6482 and 2.3 $mL \cdot min^{-1}$ for LCCF6455 at a MW power of 0.76 kW. Using the LCCF6455 fibers in the nozzle configuration demonstrates that the fibers are stable up to MW power of 1.13 kW and show a permeation of 4.6 $mL \cdot min^{-1}$. In conclusion, the nozzle configuration leads to a strong increase of both the CO_2 conversion and the permeated oxygen amount per fiber.

5. References

[1] R. Snoeckx et al., Chemical Society Reviews, **46** (19), 5805 (2017).

[2] R. Küngas, Journal of the Electrochemical Society, **167** (4), 044508 (2020).

[3] Y. Teraoka et al., Chemistry Letters, **14** (11), 1743 (1985).

[4] M. Leins et al., Journal of Visualized Experiments, **98**, 52816 (2015).

[5] K. Wiegers, Chemie Ingenieur Technik, **94** (3), 299 (2022).

[6] Buck et al., Separation and Purification Technology, **259**, 118023 (2021).

[7] Buck et al, Journal of Industrial and Engineering Chemistry, **104**, 1 (2021).

[8] A. Hecimovic et al., Journal of CO_2 Utilization, **57**, 101870 (2022).